

July 1999  
UT-KOMABA/99-9  
cond-mat/9907335

# Loop Model with Generalized Fugacity in Three Dimensions

Saburo Higuchi\*

*Department of Pure and Applied Sciences,  
The University of Tokyo, Komaba  
Komaba, Meguro, Tokyo 153-8902, Japan*

## Abstract

A statistical model of loops on the three-dimensional lattice is proposed and is investigated. It is  $O(n)$ -type but has loop fugacity that depends on global three-dimensional shapes of loops in a particular fashion. It is shown that, despite this non-locality and the dimensionality, a layer-to-layer transfer matrix can be constructed as a product of local vertex weights for infinitely many points in the parameter space. Using this transfer matrix, the site entropy is estimated numerically in the fully packed limit.

PACS: 05.20.-y 05.40.Fb 05.50.+q 36.20.-r

Keywords: self-avoiding walk; random walk;  $O(n)$  model; loop model; polymer

rcsid: \$Header: rfpl.tex,v 4.1 99/12/02 10:19:44 hig Exp \$

---

\*e-mail: hig@rice.c.u-tokyo.ac.jp

# 1 Introduction

Loop models are interesting examples of statistical models of extended objects. They are related to the  $O(n)$  spin model [1, 2], a surface growth model [3], the self-avoiding walk [4], the protein folding problem [5], and so on. It includes the fully packed loop model [6] and the Hamiltonian cycle problem [7, 8, 9] as particular limits.

The partition function of an  $O(n)$  loop model on a lattice with  $N$  sites at the inverse temperature  $x$  is given by

$$Z_{\text{loop}}(n, x^{-1}) = \sum_{c \in \mathcal{C}} x^{\mathcal{N}_S(c) - N} n^{\mathcal{N}_L(c)} \quad (n, x \in \mathbb{R}). \quad (1)$$

The summation is taken over the set  $\mathcal{C}$  of all the non-intersecting loop configurations drawn along links of the lattice. The number of loops and that of sites visited by them are denoted by  $\mathcal{N}_L(c)$  and  $\mathcal{N}_S(c)$ , respectively.

One may hope to study the model (1) by the transfer matrix approach. For  $n \in \mathbb{Z}_+$ , this is done in a simple way; one introduces link variables whose values are either occupied states with one of  $n$  colors or an unoccupied state and lets them interact on sites. A transfer matrix is written as a product of vertex weights straightforwardly.

For  $n \notin \mathbb{Z}_+$ , however, the partition sum (1) cannot be rewritten in terms of local degrees of freedom such as link variables in a simple way. It is not trivial to have a *local* transfer matrix<sup>1</sup>. I say a transfer matrix is *local* when its component is written as a product of weights each of which is determined by the local state configuration around a lattice site.

It is surprising that, in two dimensions,  $n \notin \mathbb{Z}_+$  models admit a mapping onto a state sum model with a local vertex weight and thus have local transfer matrices [10, 11, 12]. In fact, by choosing  $s \in \mathbb{C}$  satisfying  $n = s + s^{-1}$ ,  $Z_{\text{loop}}(n, x^{-1})$  can be written as

$$Z_{\text{loop}}(n, x^{-1}) = \sum_{c \in \mathcal{C}} x^{\mathcal{N}_S(c) - N} (s + s^{-1})^{\mathcal{N}_L(c)} = \sum_{c \in \bar{\mathcal{C}}} x^{\mathcal{N}_S(c) - N} \prod_{L \in \bar{\mathcal{L}}(c)} s^{\pm 1}, \quad (2)$$

where  $\bar{\mathcal{C}}$  is the set of loop configurations with a direction associated with each loop. The set  $\bar{\mathcal{L}}(c)$  consists of all the directed loops in a configuration  $c$ . A loop with the (counter-)clockwise direction is given a weight  $s^{+1}$  ( $s^{-1}$ ). This weight can be realized by associating  $s^{+1/4}(s^{-1/4})$  with each right(left)-turn site and the model can be regarded as a state sum model with a local vertex weight. This trick has made the study of two-dimensional loop models very fruitful.

Physics of loops in three dimensions is very attractive. It is realistic in the context of condensed matter physics. There has been a continuous suspicion that two-dimensional ones have missed some important ingredient in real physics, e.g. the protein folding problem. Three-dimensional loops have also rich mathematical structures. For instance, loops can be knotted or linked in

<sup>1</sup>The use of the connectivity basis is discussed in subsection 5.4.

three dimensions[13]. It is noted that a number of attractive proposals have been made to generalize the loop model to higher dimensions [14, 15].

The analysis of loop models and their generalizations in higher dimensions is, however, extremely hard to perform. Needless to say, the number of configurations increases considerably. For fugacity  $n \notin \mathbb{Z}_+$ , which includes the interesting case of the self-avoiding walk ( $n = 0$ ), no way of constructing local transfer matrices is known. This is because specialties of two dimensions cannot be used to simplify problems any more. The mapping (2) makes use of the fact that the a directed loop in two dimensions turns around just once either clockwise or counter-clockwisely. It appears that this kind of tricks never works in higher dimensions.

In this article, I propose a model which generalizes (1) in a fashion specific to three dimensions. It is furnished with loop fugacity that depends on the global three-dimensional shape of loops. I show that, despite this generalization which makes the model even more non-local, a local transfer matrix for the system can be constructed for a number of choices of fugacity. These choices include the ones that give zero or non-integer weight to loops.

This article is organized as follows. In section 2, I define a loop model in three dimensions generalizing (1). Its local transfer matrix is constructed for a family of points in the parameter space in section 3. In section 4, this transfer matrix is numerically diagonalized to yield an estimate of the site entropy in the fully packed limit  $x^{-1} = 0$ . In the last section 5, I discuss my results and their relation to combinatorial problems. In an appendix, a technical issue on the block-diagonalization of the transfer matrix is addressed.

## 2 Generalized fugacity

I define a statistical model of loops on the three-dimensional simple cubic lattice  $\mathbb{Z}^3 = \{\sum_{i=1}^3 m_i \mathbf{e}_i \in \mathbb{R}^3 | m_i \in \mathbb{Z}\}$ ,  $\mathbf{e}_i \cdot \mathbf{e}_j = \delta_{ij}$ . The partition function is given by

$$Z_{\text{loop}}[n](x^{-1}) = \sum_{c \in \mathcal{C}} x^{\mathcal{N}_s(c) - N} \prod_{L \in \mathcal{L}(c)} n(A(L)), \quad (3)$$

where  $\mathcal{L}(c)$  is the set of loops in a configuration  $c$ . The loop fugacity  $n$  is now promoted to a function which depends on the shape of  $L \in \mathcal{L}(c)$  through a quantity  $A(L) \in \mathbb{R}$  defined below.

To define  $A(L)$ , one begins with associating a closed trajectory on the unit sphere with each loop  $L$ . One picks a direction for  $L$ . On every point  $\mathbf{x} \in L \subset \mathbb{R}^3$  except for sites where  $L$  makes a turn, there is a unit tangential vector  $\mathbf{v}(\mathbf{x})$  to  $L$ ; it is either of  $\pm \mathbf{e}_i$ ,  $i = 1, 2, 3$ . One may regard  $\mathbf{v}(\mathbf{x})$  as a mapping from  $L \setminus$  ('turn-sites') to the unit sphere  $S^2$ .

As one loops along  $L$ ,  $\mathbf{v}(\mathbf{x})$  jumps from a point to another on  $S^2$ . One can naturally interpolate these points to define a continuous trajectory  $\mathbf{v} : L \rightarrow S^2$ . One has only to declare that  $\mathbf{v}(\mathbf{x})$  moves along the geodesic (of length  $\frac{1}{2}\pi$ ) on  $S^2$  at each turn-site. This is equivalent with smoothing a loop in neighborhoods

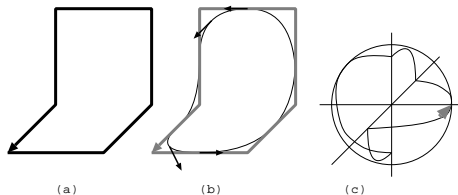


Figure 1: The definition of  $A(L)$ . (a) The original loop  $L$  with a direction associated. (b) The loop smoothed at turn-sites. (c) Trajectory of the tangent vector on the unit sphere. An area of  $A(L) = 2\pi$  is enclosed.

of turn-sites keeping it within the plane (Fig.1). Then one defines  $A(L)$  to be the oriented area encircled in the right of the trajectory  $\mathbf{v}(\mathbf{x})$ . On the lattice  $\mathbb{Z}^3$ ,  $A(L)$  takes values

$$A(L) = \frac{1}{2}m\pi \quad (m \in \mathbb{Z}). \quad (4)$$

In two dimensions, the quantity  $A(L)$  takes values  $\pm 2\pi$  and this signature corresponds to that of  $s^{\pm 1}$  in (2). Therefore (3) incorporates an essential ingredient of three-dimensional loops and is regarded as a natural generalization of (2).

As is evident from the above construction, there is certain ambiguity of the value of  $A(L)$ . First, because the trajectory is drawn on a closed surface of area  $4\pi$ ,  $A(L)$  is well-defined up to  $4\pi$ . Second, the signature of  $A(L)$  is changed when the picked direction of  $L$  is reversed. I require that  $n(\cdot)$  in (3) absorbs this ambiguity. Hence, it should satisfy

$$n(A) = n(A + 4\pi), \quad (5)$$

$$n(-A) = n(A). \quad (6)$$

Eqs. (4), (5),(6) imply that the fugacity function  $n(\cdot)$  can be specified by five parameters  $n(A)$ ,  $A = 0, \frac{1}{2}\pi, \pi, \frac{3}{2}\pi, 2\pi$ .

In spite of the above restriction on  $n(A)$ , the model (3) includes many interesting cases. Consider, for example, fugacity

$$n(A) = n_0 \delta_0^{(4)}(A), \quad (7)$$

with  $n_0 \in \mathbb{R}$  and

$$\delta_b^{(a)}(A) = \begin{cases} 1 & \text{if } (\frac{A}{\pi} - b) \equiv 0 \pmod{a}, \\ 0 & \text{otherwise.} \end{cases} \quad (8)$$

The sum in (3) is then restricted to configurations which consist only of loops with the oriented area  $A \equiv 0 \pmod{4\pi}$ . It should be interesting to compare the site entropy with that of the model with  $n(A) = n_0$ . It is also tempting to

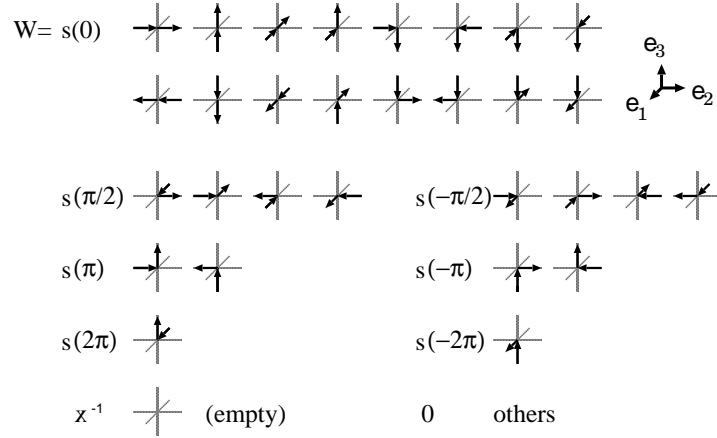


Figure 2: Vertex weights  $W$  for  $Z_{\text{vertex}}[s](x^{-1})$ .

ask whether such an additional constraint changes the critical behavior or not. The present case reminds one of the fully packed loop model in two dimensions. Its universality class differs from that of densely packed loop phase when the additional constraint that the loop length must be even is imposed [12, 16].

### 3 Transfer matrices from local vertex weights

In order to construct a local layer-to-layer transfer matrix for the loop model (3), I define a vertex model and show that it is equivalent with (3).

The local degree of freedom  $z$  of the vertex model lives on each link  $\langle \mathbf{r}, \mathbf{r} \pm \mathbf{e}_i \rangle$ ,  $\mathbf{r} \in \mathbb{Z}^3$ . It takes one of three values  $\leftarrow$ ,  $\rightarrow$ , and  $-(\text{empty})$ . On each site, six neighboring link variables interact by the vertex weight  $W$  defined in Fig. 2, where  $s(\omega)$  is a function that satisfies

$$s(A_1) \times s(A_2) = s(A_1 + A_2) \quad (9)$$

and is specified further below. The partition function of the vertex model is

$$Z_{\text{vertex}}[s](x^{-1}) = \sum_{z=\leftarrow, \rightarrow, -} \prod_{\mathbf{r} \in \mathbb{Z}^3} W(\{z(\langle \mathbf{r}, \mathbf{r} \pm \mathbf{e}_i \rangle)\}). \quad (10)$$

Evidently, the partition function (10) has a local transfer matrix which is a product of  $W$ 's.

Now I show that (10) for an appropriate  $s$  is equivalent with (3). Because the weight  $W$  is nonzero only when there is one incoming and one outgoing arrow, contribution to the partition sum (10) comes only from the set  $\bar{\mathcal{C}}$  of directed

loop configurations

$$Z_{\text{vertex}}[s](x^{-1}) = \sum_{c \in \bar{\mathcal{C}}} x^{\mathcal{N}_s(c) - N} \prod_{L \in \bar{\mathcal{L}}(c)} \left[ \prod_{\mathbf{r} \in L \cap \mathbb{Z}^3} s(\omega(\mathbf{r})) \right] \quad (11)$$

where  $s(\omega(\mathbf{r}))$  is the weight for the vertex at  $\mathbf{r} \in \mathbb{Z}^3$  in Fig.2.

The factor in the square bracket in (11) is associated with a directed loop component  $L$ . To evaluate this quantity, it is crucial to observe that

$$A(L) = \sum_{\mathbf{r} \in L \cap \mathbb{Z}^3} \omega(\mathbf{r}). \quad (12)$$

Actually, the weight system in Fig.2 is designed to have this property in refs.[17, 18, 19] in the context of random walk with a spin factor [20, 21]. Combining the properties (12) and (9), one finds that the factor in the square bracket is simply  $s(A(L))$ .

Using the same trick as that used in (2), one can further write the partition function (11) as a sum over undirected loop configurations

$$Z_{\text{vertex}}[s](x^{-1}) = \sum_{c \in \mathcal{C}} x^{\mathcal{N}_s(c) - N} \prod_{L \in \mathcal{L}(c)} (s(A(L)) + s(-A(L))). \quad (13)$$

Therefore, if  $n(A)$  in the loop model (3) can be written as

$$n(A) = s(A) + s(-A) \quad (14)$$

with a function  $s$  that satisfies (9), then the vertex model partition function  $Z_{\text{vertex}}[s](x^{-1})$  defined above is equal to (3).

The requirement (9) together with the restriction (4), (6) and (5) on  $n(A)$  forces  $s(A)$  to have a simple form

$$s(A) = e^{iJA} \quad (15)$$

with  $J \in \mathbb{Z}/2$ . It is enough [17] to consider the cases  $J = 0, \frac{1}{2}, 1, \frac{3}{2}$  and 2 because of (4). Hereafter, one introduces a shorthand notation

$$Z_J(x^{-1}) = Z_{\text{loop}}[n(A) = e^{iJA} + e^{-iJA}](x^{-1}). \quad (16)$$

The vertex weights at  $J = 0$  and 2 enjoy a special property  $s(\omega) = s(-\omega)$ . This enables one to define a model with only two microscopic states  $\leftrightarrow$  and  $-$ :

$$\begin{aligned} Z'_{\text{vertex}}[s](x^{-1}) &= \sum_{z \in \{\leftrightarrow, -\}} \prod_{\mathbf{r} \in \mathbb{Z}^3} W(\{z(\langle \mathbf{r}, \mathbf{r} \pm \mathbf{e}_i \rangle)\}) \\ &= \sum_{c \in \mathcal{C}} x^{\mathcal{N}_s(c) - N} \prod_{L \in \mathcal{L}(c)} s(A(L)), \end{aligned} \quad (17)$$

which I denote by  $Z_0'$  and  $Z_2'$ .

$J$	$n(\cdot)$
0	$2\delta_0^{(\frac{1}{2})} (\equiv 2)$
$\frac{1}{2}$	$2(\delta_0^{(4)} - \delta_2^{(4)}) + \sqrt{2}(\delta_{\frac{1}{2}}^{(4)} + \delta_{\frac{7}{2}}^{(4)} - \delta_{\frac{3}{2}}^{(4)} - \delta_{\frac{5}{2}}^{(4)})$
1	$2(\delta_0^{(2)} - \delta_1^{(2)})$
$\frac{3}{2}$	$2(\delta_0^{(4)} - \delta_2^{(4)}) - \sqrt{2}(\delta_{\frac{1}{2}}^{(4)} + \delta_{\frac{7}{2}}^{(4)} - \delta_{\frac{3}{2}}^{(4)} - \delta_{\frac{5}{2}}^{(4)})$
2	$2(\delta_0^{(1)} - \delta_{\frac{1}{2}}^{(1)})$
0'	$\delta_0^{(\frac{1}{2})} (\equiv 1)$
2'	$\delta_0^{(1)} - \delta_{\frac{1}{2}}^{(1)}$

Table 1: The generalized fugacity  $n$  which generates the semigroup of allowed models. The function  $\delta_b^{(a)}(\cdot)$  is defined in eq.(8).

The fugacity functions corresponding to  $J = 0, \frac{1}{2}, 1, \frac{3}{2}, 2, 0'$  and  $2'$  are listed in Table 1. They indeed give  $n(A) \leq 0$  or  $n(A) \notin \mathbb{Q}$  for some loops.

Although only finite number of vertex models  $J = 0, \frac{1}{2}, 1, \frac{3}{2}, 2, 0'$  and  $2'$  have been constructed above, it is possible to construct an infinite number of ones by taking the direct sum of the space of their microscopic states. More precisely, one generalizes the link variable to take one of  $2q + 1$  ( $q \in \mathbb{Z}_+$ ) states:  $\leftarrow_k, \rightarrow_k$  with the  $k$  labeling colors  $k = 1, \dots, q$  and an uncolored empty state  $-$ . Introducing parameters  $J_k \in \{0, \frac{1}{2}, 1, \frac{3}{2}, 2\}$ , the vertex weight assignments in Fig.2 are supplemented by additional rules:

- If the both two arrows have the  $k$ -th color, then  $W = e^{iJ_k\omega}$ .
- If the two colors do not agree,  $W = 0$ .

The cases  $J_k = 0', 2'$  are handled in the obvious manner.

The fugacity of the 'direct sum' model  $Z_{J_1 \oplus J_2 \oplus \dots \oplus J_q}$  is simply the sum:

$$n(A) = \sum_{k=1}^q [(e^{iJ_k A} + e^{-iJ_k A}) \times B(J_k)], \quad (18)$$

$$B(J) = \begin{cases} 1 & (J = 0, \frac{1}{2}, 1, \frac{3}{2}, 2), \\ \frac{1}{2} & (J = 0', 2'). \end{cases} \quad (19)$$

One immediately notices that

$$Z_{0' \oplus 0'} = Z_0, \quad Z_{2' \oplus 2'} = Z_2. \quad (20)$$

Thus the fugacity functions expressible via vertex models form an infinite semigroup under addition <sup>2</sup> generated by  $J = 0', \frac{1}{2}, 1, \frac{3}{2}$  and  $2'$ .

<sup>2</sup>This direct sum operation may be used for the lattice construction [17, 18, 19] of higher-spin three-dimensional field theories.

One can also take the ‘tensor product’ of the space of microscopic states of  $Z_{J_1}$  and  $Z_{J_2}$  to define a model  $Z_{J_1 \otimes J_2}$ . Let the link variable take five values  $(z_1, z_2) = \uparrow\uparrow, \uparrow\downarrow, \downarrow\uparrow, \downarrow\downarrow$ , and  $||$ . The vertex weight  $W$  is defined to be the product of  $W$ ’s with  $J = J_1$  and  $J_2$ . Then the loop fugacity becomes

$$n(A) = [(e^{iJ_1 A} + e^{-iJ_1 A}) \times B(J_1)] \times [(e^{iJ_2 A} + e^{-iJ_2 A}) \times B(J_2)]. \quad (21)$$

However, a new fugacity function cannot be realized because the partition function  $Z_{J_1 \otimes J_2}$  is equivalent with an appropriate direct sum

$$Z_{J_1 \otimes J_2} = Z_{\overline{J}_1 \oplus \dots \oplus \overline{J}_q} \quad (22)$$

corresponding to the decomposition rule of the representation of  $SU(2)$ .

## 4 Entropy estimates

I numerically diagonalize the transfer matrices constructed in section 3. Throughout this section, I concentrate on the fully packed limit  $x^{-1} = 0$  where all the sites are visited by a loop. This simple case is in fact very interesting case; in two dimensions, this limit yields a new universality class with a shifted central charge on several bipartite lattices and has been attracting much attention [16, 22, 23, 24]. It would be interesting to look at the limit where the two strong constraints are combined: the fully-packing constraint  $x^{-1} = 0$  and the constraint (7) on the shape of loops.

The site entropy in the thermodynamic limit is defined by

$$f[n](\infty) = \lim_{N \rightarrow \infty} \frac{1}{N} \log Z_{\text{loop}}[n](x^{-1} = 0). \quad (23)$$

I evaluate this quantity on quasi-one-dimensional geometry  $L_1 \times L_2 \times L_3$ ,  $L_3 \rightarrow \infty$  while  $L_1, L_2$  kept finite by calculating the largest eigenvalue of the transfer matrix in an appropriate sector.

Let  $T$  be the layer-to-layer transfer matrix in  $+\mathbf{e}_3$  (vertical) direction for the vertex model defined in (10). Then  $T$  acts on linear combinations of arrays of  $L_1 \times L_2$  vertical (colored) arrows. One can take either hard-wall or periodic boundary condition in the horizontal directions.

It is important to note that the transfer matrix  $T$  commutes with the operator giving the net flow of arrows of  $k$ -th color in  $+\mathbf{e}_3$  direction

$$d_k = (\# \uparrow_k) - (\# \downarrow_k), \quad (24)$$

which is understood as

$$d_k = (\# \uparrow_k) \bmod 2 \quad (25)$$

for  $J_k = 0'$  and  $2'$ . Thus  $T$  is block-diagonalized as

$$T = \bigoplus_{\mathbf{d}} T_{\mathbf{d}}, \quad \mathbf{d} = (d_1, \dots, d_q). \quad (26)$$



$J$	$2 \times 2(\text{h})$	$3 \times 3(\text{h})$	$3 \times 4(\text{h})$	$2 \times 2(\text{p})$	$3 \times 3(\text{p})$	$3 \times 4(\text{p})$
0	0.54202495	0.59145447	0.63524092	1.0585126	0.83841678	0.83340128
$\frac{1}{2}$	0.27123680	0.33576248	0.35050951	0.79451346	0.55900063	0.55895924
1	0.51585927	0.50234791	0.55646223	0.97170402	0.69812631	0.69832061
$\frac{3}{2}$	0.35592318	0.35908194	0.37136801	0.79451346	0.57435935	0.49496387
2	0.49499647	0.45468972	0.51615498	1.0406166	0.66200716	0.67440981
$0'$	0.46298939	0.55650697	0.60072954	0.91847381	0.79631788	0.80135760
$2'$	0.38697370	0.37695844	0.42272584	0.87898824	0.55608904	0.58497412
	$4 \times 4(\text{p})$					
$0'$	0.81947983					
$2'$	0.60931946					

Table 2: The site entropy estimated numerically.  $L_1 \times L_2$  is the size of a layer while (p) and (h) mean periodic and hard-wall boundary conditions in a layer.

The quantity (23) is obtained as

$$f[n](\infty) = \lim_{L_1, L_2 \rightarrow \infty} \frac{1}{L_1 L_2} \log |\lambda_{\mathbf{0}}^0(L_1, L_2)|, \quad (27)$$

where  $\lambda_{\mathbf{d}}^i(L_1, L_2)$  is the  $i$ -th largest eigenvalue of  $T_{\mathbf{d}}(L_1, L_2)$ . The condition  $\mathbf{d} = \mathbf{0}$  excludes unwanted configurations that have unbalanced arrows traveling along the infinite direction. Shown in Tables 2 and 3 are the finite- $L_1, L_2$  results<sup>3</sup>. The asymmetric Lanczos algorithm is utilized for the present sparse eigenproblem.

The obstacle in making  $L_1$  and  $L_2$  large in the actual numerical work is of course the exponential growth of the dimensionality of the transfer matrix. The selection of  $\mathbf{d} = \mathbf{0}$  sector helps to reduce the dimensionality, though the improvement is polynomial. For a direct sum  $Z_{J_1 \oplus \dots \oplus J_q}$ , the dimensionality is estimated to be

$$\dim(\mathbf{d} = \mathbf{0} \text{ sector}) \sim (1 + 2u + p)^{L_1 L_2} \times 2^{-p} \left( \frac{3}{4\pi L_1 L_2} \right)^{u/2}, \quad (28)$$

where  $p = \#\{k | J_k = 0' \text{ or } J_k = 2'\}$ ,  $u = q - p$ . One notices that it is better to recast  $Z_{2' \oplus 2'}$  as  $Z_2$  if one is interested in its  $\mathbf{d} = \mathbf{0}$  sector.

The exponential growth is severe even after restricting to the  $\mathbf{d} = \mathbf{0}$  sector. In order to increase  $L_1 L_2$  as much as possible within the available computer resources, I have further decomposed  $T_{\mathbf{0}}$  with respect to the eigenvalue of shift (lattice momentum) operator for the periodic boundary case where the translational symmetry is present. I have looked at the zero-momentum sector  $T_{\mathbf{0}}^{(0,0)}$  as described in the appendix A. It is quite natural to expect that the largest

<sup>3</sup>I have also measured several leading eigenvalues of  $T_{\mathbf{d}}$  with  $\mathbf{d} = (d_1, \dots, d_q)$ ,  $d_k = 0, \pm 1$ . These are related to correlation length of operators in the theory. These results will be reported elsewhere.

$\bigoplus_k J_k$	$n$	$2 \times 2(\text{h})$	$3 \times 3(\text{h})$	$2 \times 2(\text{p})$	$3 \times 3(\text{p})$
$0' \oplus 2'$	$2\delta_0^{(1)}$	0.52330515	0.57390934	1.0502400	0.81503626
$0 \oplus 0$	4	0.64498133	0.65020710	1.2354255	0.90747958
$0 \oplus 2$	$4\delta_0^{(1)}$	0.63331428	0.62765833	1.232054	0.88008432
$0' \oplus 2' \oplus 1$	$4\delta_0^{(2)}$	0.63216104	0.61664018	1.2110124	0.86121744
$0 \oplus 0 \oplus 0 \oplus 0$	8	0.76911076		1.4501153	1.0108338
$0 \oplus 0 \oplus 2 \oplus 2$	$8\delta_0^{(1)}$	1.3280134		1.4490048	0.98982172
$0 \oplus 1 \oplus 1 \oplus 2$	$8\delta_0^{(2)}$	0.75985245		1.4364447	0.97947213
$0' \oplus 2' \oplus \frac{1}{2} \oplus 1 \oplus \frac{3}{2}$	$8\delta_0^{(4)}$	0.36464934		1.3863922	0.88604978
$\frac{1}{2} \oplus \frac{3}{2}$	$4(\delta_0^{(4)} - \delta_2^{(4)})$	0.47382047	0.41770663	1.0397208	0.63630800
$0 \oplus \frac{1}{2}$	$\notin \mathbb{Q}$	0.40013109	0.54670471	1.1686609	0.84652598
$0 \oplus \frac{3}{2}$	$\notin \mathbb{Q}$	0.44457252	0.55636026	1.1686609	0.84694306
$0' \oplus 0 \oplus \frac{1}{2}$	$\notin \mathbb{Q}$	0.48094569	0.57807813	1.2520659	0.62795992
		$3 \times 4(\text{h})$	$3 \times 4(\text{p})$		
$0' \oplus 2'$	$2\delta_0^{(1)}$	0.61935581	0.81580656		

Table 3: The site entropy estimated numerically.  $L_1 \times L_2$  is the size of a layer while (p) and (h) mean periodic and hard-wall boundary conditions in a layer.

eigenvalue lies there. By this decomposition, the dimensionality of the eigenproblem is reduced, at most, by  $(L_1 L_2)^{-1}$ . As a drawback, the matrix  $T_0^{(0,0)}$  becomes less sparse than the original  $T_0$ . With both effects combined, some improvements in the memory usage and the CPU time are observed. Thus the analysis of larger systems becomes possible for the periodic boundary case, as seen in Tables 2 and 3.

## 5 Discussions

In the comparison between the periodic and the hard-wall boundary conditions, one notices that the periodic case has always larger site entropy. This is because many of the loops that wind non-trivially in the horizontal directions satisfy  $A(L) = 0$  and the loops with  $A(L) = 0$  contribute to every partition sum with a positive fugacity.

The numerical works in the present study have been carried out on modest workstations. Unfortunately, information in the thermodynamic limit  $L_1, L_2 \rightarrow \infty$  is out of reach in the present analysis. For the study of criticality, ref.[17], where random walks with the weight in Fig.2 are studied, is quite suggestive. It is reported that Euclidean symmetry is not always recovered even in the continuum limit.

I discuss relations with combinatorial problems below.

## 5.1 Even and odd number of loops of a specific type

For most allowed values of  $J$ , the loop fugacity takes both positive and negative values. Some interesting combinatorial information is encoded in these models. For example, the linear combinations  $\frac{1}{2}(Z_{0'} \pm Z_{2'})$  counts the number of loop configurations such that there are even (odd) number of loops for which  $\frac{2}{\pi}A(L) \equiv 1 \pmod{2}$ , e.g.,

$$\frac{1}{2}(Z_{0'} \pm Z_{2'}) = \begin{cases} \sum_{c \in \mathcal{C}_{\text{even}, \frac{1}{2}}} 1, \\ \sum_{c \in \mathcal{C}_{\text{odd}, \frac{1}{2}}} 1, \end{cases} \quad (29)$$

where  $\mathcal{C}_{\text{even(odd)}, a}$  is the subset of  $\mathcal{C}$  and is defined by the following properties.

- $c \in \mathcal{C}_{\text{even(odd)}, a}$  contains even (odd) number of loops with  $A(L)/a\pi \equiv 1 \pmod{2}$ .
- All other loops in  $c \in \mathcal{C}_{\text{even(odd)}, a}$  satisfy  $A(L)/a\pi \equiv 0 \pmod{2}$ .

Similarly, the quantities  $\frac{1}{2}(Z_{0' \oplus 2'} \pm Z_1)$  and  $\frac{1}{2}(Z_{0' \oplus 2' \oplus 1} \pm Z_{\frac{1}{2} \oplus \frac{3}{2}})$  are interpreted as the sums over  $\mathcal{C}_{\text{even(odd)}, 1}$  and  $\mathcal{C}_{\text{even(odd)}, 2}$ .

Of the two  $Z$ 's in (29), the one with the larger leading eigenvalue dominates the sum in the limit  $L_3 \rightarrow \infty$  studied in section 3. In finite geometries, both terms contribute to yield an exact number.

## 5.2 Self-avoiding walk

The partition function (1) in the limit  $n \rightarrow 0$  corresponds to the enumeration of self-avoiding walks. Self-avoiding walks in three-dimensions have mainly been studied by the exact enumeration method due to the lack of transfer matrix formalism as pointed out in the introduction.

The model I propose in this paper can be regarded as a step forward to overcome this difficulty; in the models  $Z_{0' \oplus 2'}$ ,  $Z_{0' \oplus 2' \oplus 1}$  and  $Z_{0' \oplus 2' \oplus \frac{1}{2} \oplus 1 \oplus \frac{3}{2}}$ , the fugacity is set zero for families of loops. This is, however, achieved by paying the cost of having larger  $n$  for another family of loops. Within the present construction, loops with  $A(L) \equiv 0 \pmod{4\pi}$  cannot have weights different from the number of possible link states. Thus the partition function listed above serve only as a very loose upper bound for the entropy of self-avoiding walks.

The problem of construction of a local transfer matrix to enumerate self-avoiding walks on three-dimensional lattices still remains open.

## 5.3 Mapping to ribbon configurations

The oriented area defined in (3) has a nice geometric interpretation as holonomy. The tangent vector  $\mathbf{v}(\mathbf{x})$  moves along a trajectory on  $S^2$ . Let the unit vector tangential to this trajectory at  $\mathbf{v}(\mathbf{x}_0)$  be  $\mathbf{u}_0$  (Fig.3). Consider the parallel transport (in the sense of riemannian geometry) of  $\mathbf{u}_0$  along the trajectory  $\mathbf{v}(\mathbf{x})$  on  $S^2$ .

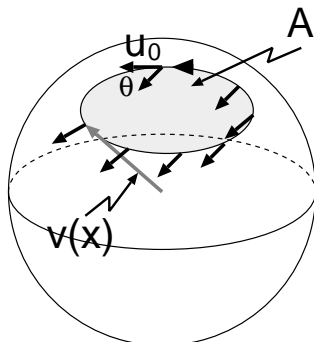


Figure 3: When  $\mathbf{u}_0$ , the tangent vector at  $\mathbf{v}(\mathbf{x}_0)$ , is parallel-transported along the trajectory on  $S^2$ , it receives holonomy whose magnitude (angle  $\theta$ ) is equal to the oriented area  $A(L)$  the path encloses.

When  $\mathbf{u}_0$  is transported back to  $\mathbf{v}(\mathbf{x}_0)$ , it gains some holonomy ( the angle  $\theta$  in Fig.3). This holonomy angle is given by the integration of the scalar curvature of  $S^2$  over the domain encircled by the trajectory and is nothing but the oriented area  $A(L)$ . In the real space  $\mathbb{Z}^3 \subset \mathbb{R}^3$ , the holonomy described above is nicely kept track of by broadening the loop segment to a ‘ribbon’ with the distinction of the right and the reversed sides. The parallel transportation can be recasted as a rule of bending ribbons on sites, which is shown in Fig.4. Among the loop configurations shown in Fig.4, the partition sum  $Z_{\text{loop}}$  with fugacity  $n = \delta_0^{(2)}$ ,  $\delta_0^{(1)}$  and  $\delta_0^{(\frac{1}{2})}$  receives contribution from  $\{(a)\}$ ,  $\{(a),(b)\}$ , and  $\{(a),(b),(c)\}$ , respectively.

For  $n = 4\delta_0^{(2)}$ , the sum in (3) is over ribbon loop configurations without mismatch. In that interpretation, the coefficient four is naturally regarded as the number of directions the right side can face. Therefore,  $Z_{\text{loop}}[n = 4\delta_0^{(2)}](x^{-1})$  is nothing but the generating function of the number of allowed ribbon configurations<sup>4</sup>.

Similarly, the partition sum for  $n = 2\delta_0^{(1)}$  can be interpreted as the sum over the configurations of ribbons without the distinction between the right and the reverse sides, while in the case  $n = \delta_0^{(\frac{1}{2})}$ , the loop segment is just a chord. This interpretation suggests that (3) may be regarded as a model of polymers with various partially broken axial symmetry by, for instance, the presence of side chains.

---

<sup>4</sup>This observation clearly indicate a simple way of constructing transfer matrices for this fugacity function. The link variable represents the ribbon which can be placed in four ways. The rule of bending is implemented in the vertex weight. The construction in section 3, however, has an advantage; the size of the matrix can be reduced more by the choice of the sector  $\mathbf{d} = \mathbf{0}$ .

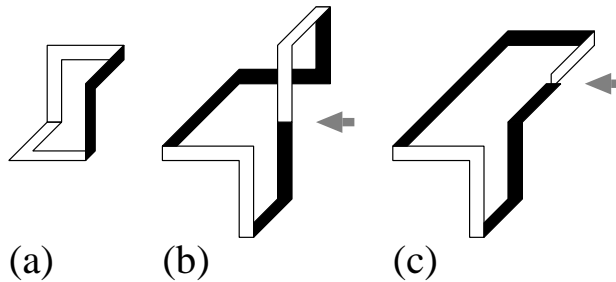


Figure 4: Examples of allowed ways of bending ribbons at sites (except for the ones indicated by gray arrows) The holonomy is accumulated at the sites indicated by gray arrows. The right and the reverse sides of ribbons are represented by white and black colors.

#### 5.4 Comparison with the connectivity basis

The connectivity basis[25, 26] is very powerful in that one can always write a transfer matrix for a loop model with respect to it. It has been very useful for numerical calculation in two-dimensions.

Nevertheless, I have avoided the use of the connectivity basis in the present work. The reason is the following. First, its fundamental degrees of freedom are not the link variables and the transfer matrix with respect to it is not local. Local transfer matrices have merits even in two dimensions. Namely, it paved the way to the Bethe ansatz solution[27, 28] and the conformal field theoretic description [29, 30] via Coulomb gas representation. Second, in three dimensions and higher, the size of connectivity basis grows considerably because of the lack of the planarity constraint. It is not clear if it is effective to perform numerical calculation in this basis. In two dimensions, the present basis is as good as the connectivity one [12, 22].

I suppose it is very important to see how useful the connectivity basis in three dimensions is and to try to improve the efficiency of the calculation in that basis.

### Acknowledgments

thank S. Tanimura for useful discussions on geometric phases. I gratefully acknowledge useful conversations with M. Asano, E. Gutter, C. Itoi, S. Hikami, K. Minakuchi, and J. Suzuki. I thank T. Iwai and Y. Uwano for discussions and for hospitality at Kyoto University, where a part of this work was done.

This work was supported by the Ministry of Education, Science and Culture under Grant 08454106 and 10740108 and by Japan Science and Technology Corporation under CREST.

## A Projection to zero momentum subspace

In this short note, I describe the block-diagonalization of the transfer matrix with respect to the eigenvalues of the lattice momentum operators. The zero-momentum subspace and a reduced transfer matrix which acts on it are explicitly constructed<sup>5</sup>.

One may start with the  $(2q + 1)^{L_1 L_2}$ -dimensional whole space of colored arrow configurations or an eigenspace of the operator  $\mathbf{d}$ . One considers the matrix elements in the basis  $u_i, (i = 1, \dots, m)$ , each of which represents a single arrow configuration such as  $\uparrow\downarrow | \dots \uparrow | \downarrow$ :

$$T u_i = \sum_{j=1}^m T_i^j u_j. \quad (30)$$

In this natural basis, the matrix  $T$  becomes sparse.

Let  $S_1$  and  $S_2$  be discrete shift operators in the horizontal directions. Then the vectors

$$v_j = \sum_{a=0}^{L_1-1} \sum_{b=0}^{L_2-1} (S_1)^a (S_2)^b u_j \quad (31)$$

are zero-momentum ones.

One classifies the index set as  $\{1, \dots, m\} = \sqcup_{I=1}^M V_I$  by an equivalence relation  $i \sim j \Leftrightarrow v_i = v_j$ . Then  $I = 1, \dots, M$  labels the zero-momentum subspace. The  $(I, J)$ -component of the block matrix is simply

$$(T_{\mathbf{0}}^{(0,0)})_I^J = \sum_{j \in V_J} T_i^j \quad (i \in V_I). \quad (32)$$

This procedure is fairly easy to implement in the sparse algorithm.

Evidently, a slight modification of the above procedure enables one to focus on a chosen non-zero momentum subspace. It will be useful for identifying excited states.

It is noted that the above block-decomposition can be applied even if the seam factor is present, *e.g.* to two-dimensional  $O(n)$  model with cylinder topology. One can make the system translationally invariant by distributing the seam factor among all horizontal links. I have checked that this prescription improves the efficiency of the the enumeration of Hamiltonian cycles performed in ref.[22] although the weight system becomes system size dependent.

## References

- [1] B. Nienhuis, Exact critical point and critical exponents of  $O(n)$  model in two dimensions, *Phys. Rev. Lett.* **49** (1982) 1062.

---

<sup>5</sup>It may well improve the efficiency just to choose a zero-momentum state as the initial Lanczos vector in the sparse algorithm without explicitly constructing a transfer matrix in the subspace as is done in the text.

- [2] E. Domany, D. Mukamel, B. Nienhuis, and A. Schwimmer, duality relations and equivalences for models with  $O(n)$  and cubic symmetry, *Nucl. Phys.* **B190** (1981) 279.
- [3] J. Kondev and C. L. Henley, Four-coloring model on the square lattice: A critical ground state, *Phys. Rev.* **B52** (1995) 6628.
- [4] B. Duplantier and H. Saleur, Exact critical properties of two-dimensional dense self-avoiding walks, *Nucl. Phys.* **B290**[FS20] (1987) 291.
- [5] H. S. Chan and K. A. Dill, Compact polymers, *Macromolecules* **22** (1989) 4559.
- [6] H. W. J. Blöte and B. Nienhuis, Fully packed loop model on the honeycomb lattice, *Phys. Rev. Lett.* **72** (1994) 1372.
- [7] H. Orland, C. Itzykson, and C. de Dominicis, An evaluation of the number of Hamiltonian paths, *J. Physique* **46** (1985) L353.
- [8] J. Suzuki, Evaluation of the connectivity of Hamiltonian paths on regular lattices, *J. Phys. Soc. Japan* **57** (1988) 687.
- [9] S. Higuchi, Field theoretic approach to the counting problem of Hamiltonian cycles of graphs, *Phys. Rev.* **E58** (1998) 128, cond-mat/9711152, (link to AIP server).
- [10] R. J. Baxter, Colorings of a hexagonal lattice, *J. of Math. Phys.* **11** (1970) 784.
- [11] B. Nienhuis, Coulomb gas formulation of two-dimensional phase transitions, in *Phase transitions and critical phenomena*, edited by C. Domb and J. Lebowitz, volume 11, pages 1–53, Academic Press, 1987.
- [12] M. T. Batchelor, H. W. J. Blöte, B. Nienhuis, and C. M. Yung, Critical behaviour of the fully packed loop model on the square lattice, *J. Phys. A* **29** (1996) L399.
- [13] S. K. Nechaev, *Statistics of knots and entangled random walks*, World Scientific, Singapore, 1996, cond-mat/9812205.
- [14] K. J. Wiese and M. Kardar, A geometric generalization of field theory to manifolds of arbitrary dimension, *Eur. Phys. J.* **B7** (1998) 187, cond-mat/9803279.
- [15] K. J. Wiese and M. Kardar, Generalizing the  $O(N)$ -field theory to  $N$ -colored manifolds of arbitrary internal dimension  $D$ , *Nucl. Phys.* **B528** (1998) 469, cond-mat/9803389.
- [16] J. L. Jacobsen, On the universality of compact polymers, *J. Phys. A* **32** (1999) 5445, cond-mat/9903132.

- [17] M. Asano, C. Itoi, and S.-I. Kojima, Random walk construction of spinor fields on three-dimensional lattice, *Nucl. Phys.* **B448** (1995) 533, hep-th/9412215.
- [18] M. Asano, C. Itoi, and S.-I. Kojima, Quantum diffusion process with a complex weight on three-dimensional lattice, in *Proceedings to the International Seminar Devoted to the 140th Birthday of Henri Poincaré*, Protovino, Russia, 1994, IHPE, hep-th/9410090.
- [19] C. Itoi, Smooth paths on three-dimensional lattice, *Phys. Rev. Lett.* **73** (1994) 3335, hep-th/9406123.
- [20] A. M. Polyakov, Fermi-Bose transmutations induced by gauge fields, *Mod. Phys. Lett.* **A3** (1988) 325.
- [21] S. Iso, C. Itoi, and H. Mukaida, Geometric description for spinning particles in three dimensions and Chern-Simons-Polyakov theory, *Phys. Lett.* **B236** (1990) 287.
- [22] S. Higuchi, Compact polymers on decorated square lattices, *J. Phys. A* **32** (1999) 3697, cond-mat/9811426, (link to IOP server).
- [23] P. Di Francesco, E. Guitter, and C. Kristjansen, Fully packed  $O(n = 1)$  model on random Eulerian triangulations, *Nucl. Phys.* **B549[FS]** (1999) 657, cond-mat/9902082.
- [24] E. Guitter, C. Kristjansen, and J. L. Nielsen, Hamiltonian cycles on random Eulerian triangulations, *Nucl. Phys.* **B546[FS]** (1999) 731, cond-mat/9811289.
- [25] T. G. Schmalz, G. E. Hite, and D. J. Klein, Compact self-avoiding circuits on two-dimensional lattices, *J. Phys. A* **17** (1984) 445.
- [26] H. W. J. Blöte and B. Nienhuis, Critical behaviour and conformal anomaly of the  $O(n)$  model on the square lattice, *J. Phys. A* **22** (1989) 1415.
- [27] R. Baxter, *Exactly solvable models in statistical mechanics*, Academic Press, London, 1982.
- [28] M. T. Batchelor and H. W. Blöte, Conformal anomaly and scaling dimensions of the  $O(n)$  model from an exact solution on the honeycomb lattice, *Phys. Rev. Lett.* **61** (1988) 138.
- [29] J. Cardy, Geometrical properties of loops and cluster boundaries, in *Fluctuating geometries in statistical mechanics and field theory*, edited by F. David, P. Ginsparg, and J. Zinn-Justin, Les Houches Session LXII, Elsevier, 1994, cond-mat/9409094.
- [30] J. L. Jacobsen and J. Kondev, Field theory of compact polymers on the square lattice, *Nucl. Phys.* **B532[FS]** (1998) 635, cond-mat/9804048.